

Parameters Affecting Performance Of Arsenic Adsorption By Magnetic Graphene Oxide

Ali Ibrahim Sherlala^a, Abdelbasat A.Kazouri^b, Nasser Abushrenta^c

^aChemical Engineering Department, Faculty of Engineering Technology-Janzour, Tripoli, Libya

^b Chemical Engineering Department, Faculty of Engineering Technology-Janzour, Tripoli, Libya

^c Chemical Engineering Department, Elmergib University, Faculty of Engineering Garaboulli, Al-khoms, Libya

***Corresponding author:**

E-mail address: sherlalaali@gmail.com

ABSTRACT: Water is the most essential substance for all life on earth and a precious resource for human civilization. Reliable access to clean and affordable water is considered one of the most basic humanitarian goals and remains a major challenge for the 21st century. Adsorption is one of the most effective approach to clean water by removing toxic pollutants. Grapheme oxide/Iron oxides hybrid are recently used by few researchers for the purpose of removing arsenic from waste water

In this study, Magnetic graphene oxide was synthesized by co-precipitation method and used as an adsorbent for arsenic removal from aqueous solution. The structures and properties of the grapheme oxide, magnetic grapheme oxide was investigated by X-ray diffraction, Fourier transformed infrared spectroscopy, FTIR. Batch laboratory tests were conducted to evaluate removal efficiency. Additionally, as (III) adsorption capacity of synthesized materials were studied. The highest percentage of removal is obtained between pH7.5 and 10.5.

Key words: Graphene oxide, Magnetic graphene oxide, Adsorption, Arsenic, Water treatment.

1. INTRODUCTION.

With rapid increase in world's population and continued industrialization, the world is facing an acute problem of wastewater management and its recovery. Industrial activities such as electroplating, mining, refinery, printing, dyeing and tanning discharge effluents, which contain heavy metals and other recalcitrant organic pollutants (1). Unlike organic pollutants, heavy metals are stable and possess low levels of biodegradability (2). Therefore, heavy metals stay stable in the environment and accumulate in the soil, water and the food chain at toxic levels due to long term exposure to wastewater discharge (3). Chronic indigestion of arsenic is known to have carcinogenic, dermatological, cardio renal and gastrointestinal effects (4). Therefore, industrial

effluents require effective treatment to control heavy metal concentrations below permissible levels before being discharged into water bodies,

Graphene, a two-dimensional carbon-based material with one atom thickness, is commonly used adsorbent due to their unique physical and chemical properties. Other excellent properties of graphene include its lamellar structure, high surface area and ease of synthesis (5). However, in many applications, surface modification is necessary as normal graphene may be ineffective in some specific applications such as adsorption of metal ions (6). Alternatively, Graphene oxide (GO), which exhibits large surface area, chemical stability and rich functional groups, has proven an effective sorbent for the removal of heavy metal ions. However, it is difficult to separate it from aqueous solutions as it usually dispersed in the aqueous solution because of its small particle size (7). Therefore, MGO Nano-hybrids have been synthesized that exhibit excellent adsorption capacities for the removal of heavy metal in aqueous solution. Beside post separation of adsorbent was considered.

The aim of this work is therefore to synthesize iron oxide-graphene oxide for arsenic removal. Also, of various experimental parameters on adsorption process performance, such as effluent pH, temperature, adsorbent dose and contact time was studied in details.

2-Experimental

2.1 Chemicals

All chemicals used were of analytical reagent grade and used without further purification. Graphite powder (particle size <20 μm) was obtained from Sigma Aldrich- Malaysia. Other chemicals such as Ferric chloride (99%), Ferrous chloride (99%), Potassium Permanganate (99%), Ammonia solution (30%), Hydrogen Peroxide (30% w/v) and Sodium Arsenite (98.5%) was procured from R&M marketing Essex UK. Deionized water was used for samples preparation.

2.2 Synthesis of Graphene oxide

2.2.1 Synthesis of the adsorbent

Graphene oxide (GO) was synthesized according to improved Hummer's method (8). A graphite powder (3.0 g) was mixed with concentrated H_2SO_4 (70 ml) in an ice bath. Under vigorous agitation, $KMNO_4$ (9.0 g) was added slowly to keep the temperature of the suspension lower than 20 °C. Subsequently, the reaction system was transferred to oil bath which was maintained at 40 °C. The reaction mixture was vigorously stirred for 30 minutes. Subsequently, 150 ml of the water was added and solution was stirred for 15 min at 95 °C. Later, 500 ml of water was added followed by the slow addition of 15 ml H_2O_2 . As a result, the colour of the solution was turned from dark brown to yellow. The resulting mixture was filtered and washed with 1:10 HCl aqueous solution (250 ml). The filtered solids were dried in air and as a result graphene oxide (GO) powder was obtained

2.2.2 Synthesis Of iron Oxide

Iron oxides were prepared by chemical precipitation. 2.43 g of $FeCl_3$ and 0.99 g of $FeCl_2$ were dissolved in 80 ml of deionized water and mixed properly. Subsequently, 6 ml of ammonia solution was added and sonicated for 1 h. The resulting mixture was decanted, washed two time with deionized water and separated again. The separated solids were dried in oven at 50°C. (9)

2.2.3 Synthesis of magnetic graphene oxide

The iron oxide particles were mixed with 0.2 g of graphene oxide in 50 ml of deionized water. The mixture was stirred for 18-24 h and centrifuged. The separated solid content was washed and centrifuged. The process was repeated two times and dried in oven at 50 °C to obtain GO/Iron oxide binary oxide (10).

2.3. Characterization

The morphologies of the synthesized adsorbent were characterized. The crystalline phase of iron oxide was investigated using X-ray diffraction (XRD) technique. Fourier Transform Infrared spectroscopy FTIR was used to study the functional groups of the adsorbents within the frequency range of 4000-400cm⁻¹. The concentration of arsenic in the aqueous solution was determined using Inductively coupled plasma mass spectroscopy (ICP Optima 7000 DV, Perkin Elmer).

2.4. Experimental Procedure

The adsorption of arsenic (III) was performed in a batch experiment. 0.1-0.5 gram of synthesized adsorbents added to 100 ml of arsenic solution at desired concentrations. The arsenic solution was prepared using a deionized Millipore water. The mixture was stirred and pH of the solution was adjusted according to the desired value by adding 1.0 M NaOH or 1.0 M HNO_3 . The stirring time was also varied accordingly. After a desired time, the solid phase was removed from the supernatant by decantation with magnet and centrifuge at 4000 rpm for 30 min. Arsenic content in the obtained supernatant is determined by ICP. After separation, the treated solution was sampled and analysed to determine the arsenic removal.

efficiency. The removal efficiency was calculated according to equation.

$$\text{Adsorption efficiency (\%)} = \frac{C_o - C_e}{C_o} \times 100$$

Where C_o and C_e are the initial and equilibrium concentrations of arsenic in the solution (mg/L).

3. Results and discussion

3.1. Characterization of MGO

3.1.1 XRD Analysis

X-ray powder diffraction is a rapid technique primarily to identify crystalline phase and degree of crystallinity of thin films and powder. diffraction pattern allows the detection of phase composition and texture of the adsorbent, favoured orientation and size of crystallites. Figure 1 shows the X-ray diffraction (XRD) patterns of the natural graphite, the GO, IO-GO, for original graphite, the characteristic (002) diffraction peak appears at around $2\theta = 27$ (Figure 1a).

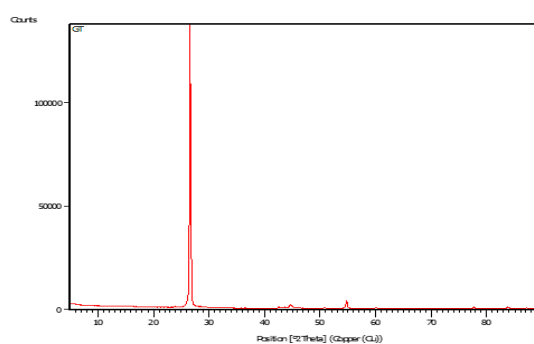


Figure 1(a) XRD pattern for Graphite

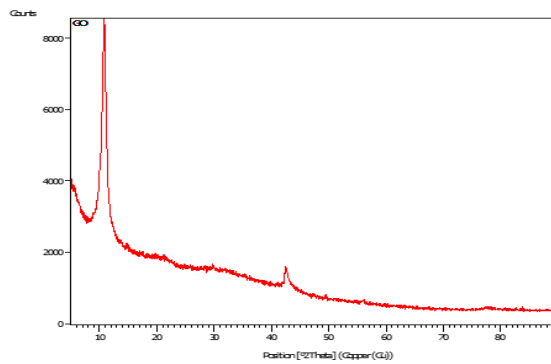


Figure 1 (b) XRD pattern for Graphene

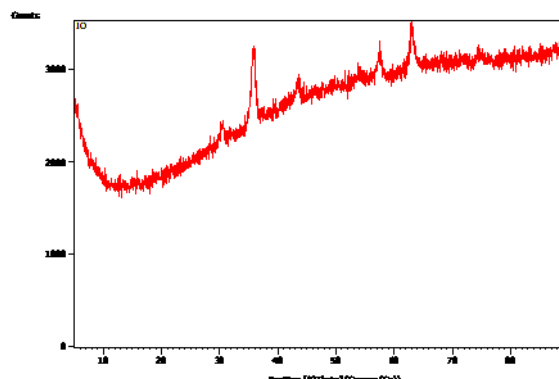


Fig.1(c) XRD pattern for Graphene oxide

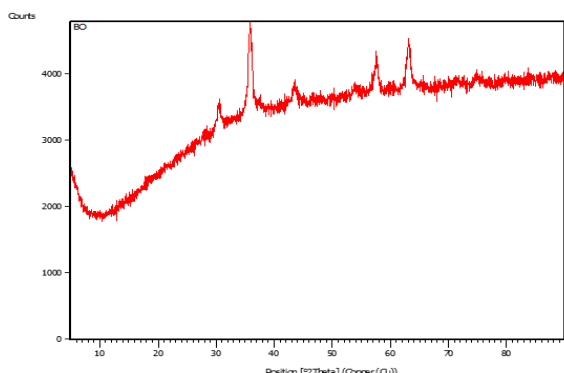


Fig. 1 (d) XRD pattern for magnetic graphene oxide

After oxidation, this diffraction peak shifted to a lower angle around 11 (Figure 1b) indicating the introduction of oxygen-containing groups to form the GO. Compared with the pure GO and graphite signals, there were no diffraction signals belonging to the GO sheets in IO-GO. This result was ascribed to the formation of iron oxides crystals between the layers of GO, which might destroy the regular layer stacking of GO and exfoliate the GO nanosheets, resulting in the disappearance of the GO signal (11).

3.1.2. FTIR Analysis

Figure 2 presents the FT-IR spectra of Fe_2O_3 /Graphene and graphene oxide. The peak intensity of some oxygen-containing groups, such as C-OH (3400 cm^{-1}), C=O (1730 cm^{-1}) and C-O-C (1220 cm^{-1}) (12) show obvious decreases for Fe_2O_3 /Graphene compared with that of graphene oxide, indicating the reduction of graphene oxide in great degree. However, apart from weakening intensity of C=O peak at 1730 cm^{-1} , the peak intensity of other oxygen-containing groups for Fe_2O_3 /Graphene. It suggests the reduction of GO should be attributable. Additionally, intense peaks located at 1640 cm^{-1} , 1050 cm^{-1} and 1400 cm^{-1} are resulted from the skeptical vibration of graphitic domains, C-O stretching and O-H deformation peak respectively, while the sharp peaks observed at 480 cm^{-1} and 577 cm^{-1} could be assigned to the stretching vibration of Fe-O bonds (13-16).

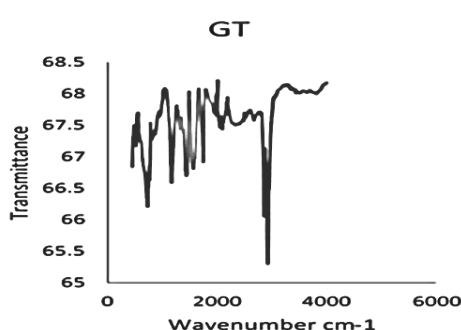


Fig. 2 (a) FTIR spectrum for Graphite

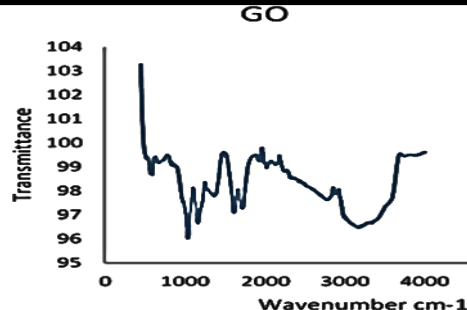


Fig. 2 (b) FTIR spectrum for Graphene oxide

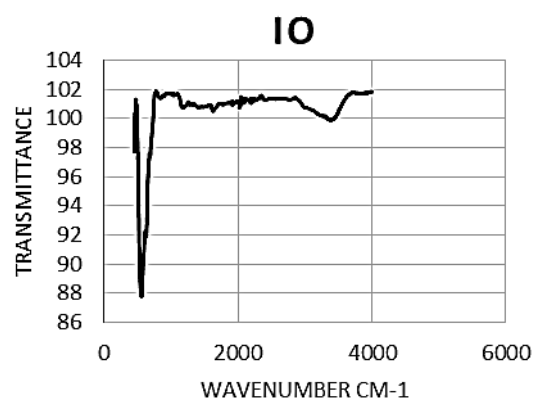


Fig. 2 (c) FTIR spectrum for Iron oxide

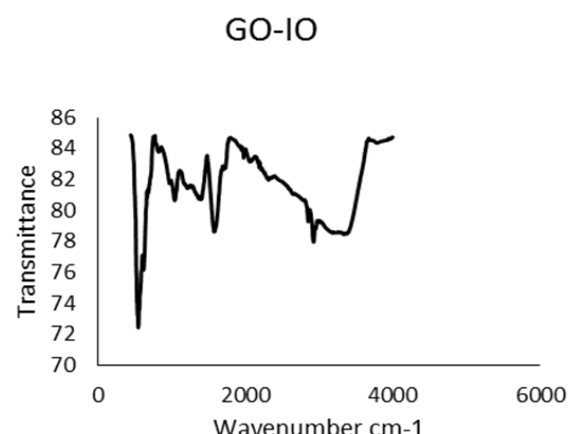


Fig. 2 (d) FTIR spectrum for Graphene oxide – Iron oxide

3.2. Adsorption studies

Effect of various parameters on arsenic adsorption

3.2.1. pH effect

The solution pH is one of the most important parameters for the metal solution because of its remarkable effect on the speciation of metal ions, the surface charge and the binding sites of the sorbent. In the present work, effect of pH on adsorption of As(III) was studied at different pH ranging

from 2.5 to 11.5, keeping all other parameters fixed, that is, (adsorbent dose = 1.2 g/L, As (III) concentration = 250 $\mu\text{g/L}$, pH = 7.0, and contact time = 6 h).

Adsorption percentage varies with the variation in pH of the solutions. It is disclosed that removal % increased from 28.5% to 61.5% from pH values 2–7.5. The highest percentage of removal is obtained between pH 7.5 and 10.5. This can be explained by the existing species of as (III), the surface charge and functional groups on the composite. The decrement was seen in the percentage removal when the pH values move towards basicity (Figure 3). The highest removal efficiency was observed from 7 to 9.5 pH values, that is, pH of groundwater. Since As (III) exists in neutral unionized form (H_3AsO_3) below pH 9, electrostatic interaction between the metal species and the functional group adsorbent is therefore unlikely. Thus, other mechanisms must be responsible for the adsorption in these pH conditions.

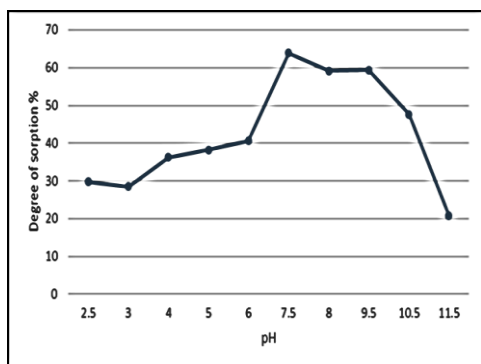


Fig. 3 Effect of pH on Arsenite adsorption (adsorbent dose = 1.2 g/L, as (III) concentration = 250 $\mu\text{g/L}$, and contact time = 6 h).

For As (III), as pH value increases, the amount of negatively charged arsenic, which suggests that the electrostatic factors do not sole control the adsorption process onto MGO, surface complexation mainly played an important role in the adsorption process. In Figure 3, the adsorption amount of as (III) increases with increasing pH from 2.5 to 6.1, when pH is in the 7.5–9.5 range, the adsorption amount nearly remains unchanged, but when pH above 9.5, the adsorption amount of as (III) increases, attitudes to surface complexation. The initial increase in the adsorption efficiency with increasing pH may have been due to the presence of more OH groups at the surface of the nano composites (8). The sharp decrease in the removal efficiency above pH 9.7 is likely due to the electrostatic repulsion between the negatively charged surface of the MGO and the deprotonated anionic arsenic (17). It can be concluded, based on the foregoing, that the adsorption of as (III) by MGO is not controlled by electrostatic interactions. Although the adsorption of as (III) is mainly attributed to surface complexation, the exact mechanism is still open to discussion (18).

3.2.2 Adsorbent dosage

Adsorbent dosage is an important parameter which determines the number of potential active sites for the pollutants. The dosage was varied between 0.052 and 0.25 g/L. It can be seen from Figure (4) that as the dosage increases from 0.025 to 0.22314 g/L, the arsenic removal increases to about 70.78%. However, the removal efficiency decreased when the adsorbent dosage was increased above 0.0223 g/L, indicating an optimum dosage around that point. As the adsorbent dosage increases, more active sites for adsorption become available and the rate of arsenic removal increases. However, excess adsorbent dosage can lead to overlapping and stacking of the active sites of adsorption and hence, the decreased in the arsenic removal (20). This may explain the decrease in the efficiency of the process as the dosage was increased beyond 0.02234 g/L in this study.

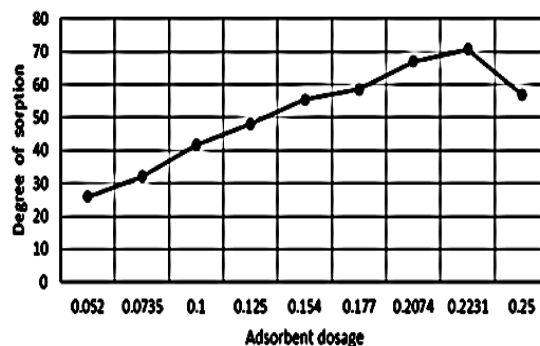


Fig. 4 Effect of Adsorbent dosage on Arsenite removal efficiency (As (III) concentration=250 $\mu\text{g/L}$, pH =7.0, and contact time = 6 h).

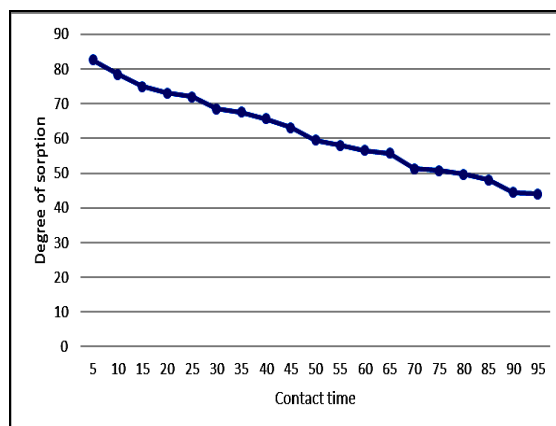


Fig. 5 Effect of contact time on Arsenite removal efficiency (adsorbent dose = 1.2 g/L, as (III) concentration = 250 $\mu\text{g/L}$, pH = 7.0).

3.2.4. Contact time

The effect of contact time was investigated between 5 and 95 min. It can be seen from Figure (5) that the arsenic removal decreases with increase in the contact time. The adsorption process was very fast in the first 5 min, and then proceeded slowly. For example, more than 80% was achieved after the first 5 min and this decreased to only about 44% after 95 min. At the beginning of the process,

large active sites for adsorption are available and the adsorbent could adsorb most of the As (III) very fast. However, as the adsorption proceeds, the active surfaces are filled up and the adsorption process slowed down until equilibrium is reached. A similar two-stage adsorption process had been reported earlier (19). Up pal et al. had reported a similar observation in their study for arsenic adsorption using zinc peroxide functionalized GO (20).

4. Conclusion

The following points are derived from the study:

1. Iron oxide, graphene oxide and iron oxide-graphene oxide composite have been successfully synthesized as verified by XRD, FTIR analysis.
2. Iron oxide is the dominant compound in the composite.
3. Based on the foregoing, that the adsorption of As (III) by MGO is not controlled by electrostatic interactions. Although the adsorption of As (III) is mainly attributed to surface complexation, the exact mechanism is still open to discussion.
4. As the adsorption proceeds, the active surfaces are filled up and the adsorption process slowed down until equilibrium is reached.
5. Aggregation of adsorbent may interpret the decrease of removal efficiency of As (III) beyond adsorbent dosage of 0.0223 g/L.

ACKNOWLEDGMENTS

This work was supported by the University of Malaya Postgraduate Research Grant Number PG086-2016A.

References.

- [1] Majumdar, S. S., Das, S. K., Saha, T., Panda, G. C., Bandyopadhyoy, T., & Guha, A. K. (2008). Adsorption behavior of copper ions on *Mucor rouxii* biomass through microscopic and FTIR analysis. *Colloids and Surfaces B: Biointerfaces*, 63(1), 138-145. doi: <http://dx.doi.org/10.1016/j.colsurfb.2007.11.022>
- [2] Hegazi, H. A. (2013). Removal of heavy metals from wastewater using agricultural and industrial wastes as adsorbents. *HBRC Journal*, 9(3), 276-282. doi: <http://dx.doi.org/10.1016/j.hbrcj.2013.08.004>
- [3] Amin, N.-u., & Ahmad, T. (2015). Contamination of soil with heavy metals from industrial effluent and their translocation in green vegetables of Peshawar, Pakistan. *RSC Advances*, 5(19), 14322-14329. doi: 10.1039/C4RA14957B
- [4] Chen, X., Yang, L., Zhang, J., & Huang, Y. (2014). Exploration of As(III)/As(V) Uptake from Aqueous Solution by Synthesized Calcium Sulfate Whisker. *Chinese Journal of Chemical Engineering*, 22(11-12), 1340-1346. doi: <http://dx.doi.org/10.1016/j.cjche.2014.09.018>
- [5] Cortés-Arriagada, D., & Toro-Labbé, A. (2016). Aluminum and iron doped graphene for adsorption of methylated arsenic pollutants. *Applied Surface Science* 386, 8495. doi: <http://dx.doi.org/10.1016/j.apsusc.2016.05.154>
- [6] Cao, Y., & Li, X. (2014). Adsorption of graphene for the removal of inorganic pollutants in water purification: A review.
- [7] Ramesha, G. K., Vijaya Kumara, A., Muralidhara, H. B., & Sampath, S. (2011). Graphene and graphene oxide as effective adsorbents toward anionic and cationic dyes. *J Colloid Interface Sci*, 361(1), 270-277. doi: <http://dx.doi.org/10.1016/j.jcis.2011.05.050>
- [8] Chen, J., Yao, B., Li, C., & Shi, G. (2013). An improved Hummers method for eco-friendly synthesis of graphene oxide. *Carbon*, 64, 225-229.
- [9] Pirouz, A. A., Karjiban, R. A., Bakar, F. A., & Selamat, J. (2018). A Novel Adsorbent Magnetic Graphene Oxide Modified with Chitosan for the Simultaneous Reduction of Mycotoxins. *Toxins*, 10, 1-13.
- [10] Sherlala AIA, Raman AA, Bello MM. Adsorption of arsenic from aqueous solution using magnetic graphene oxide. *IOP Conf Ser Mater Sci Eng*. 2017;210:1-8
- [11] Y. Fu, P. Xiong, H. Chen, X. Sun, X. Wang, High photocatalytic activity of agnetically separable manganese ferrite-grapheneheteroarchitectures, *Ind. Eng. Chem. Res.* 51 (2012) 725-731
- [12] Jain, A., Raven, K. P., & Loepert, R. H. (1999). Arsenite and arsenate adsorption on ferrihydrite: Surface charge reduction and net OH-release stoichiometry. *Environmental Science and Technology*, 33, 1179-1184.,
- [13] Jiang, Y., Gong, J. L., Zeng, G. M., Ou, X. M., Chang, Y. N., Deng, C. H., ... Huang, S. Y. (2016). Magnetic chitosan-graphene oxide composite for anti-microbial and dye removal applications. *International Journal of Biological Macromolecules*, 82, 702-710.
- [14] Kalel, N., Rahim, A., Yusoff, M., Krishna, S., Abdul, Z., & Salmiati, S. (2017). High concentration arsenic removal from aqueous solution using nano-iron ion enrich material (NIIEM) super adsorbent. *Chemical Engineering Journal*, 317, 343-355.
- [15] Khatamian, M., Khodakarampoor, N., & Saket-Oskoui, M. (2017). Efficient removal of arsenic using graphene-zeolite based composites. *Journal of Colloid and Interface Science*, 498, 433-441.
- [16] Chen, A. W., Zeng, G. M., Liu, S. M., ... Liu, S. H. (2013). Removal of Cu(II) ions from aqueous solution using sulfonated magnetic graphene oxide composite. *Separation and Purification Technology*, 108, 189-195.
- [17] Boddu, V. M., Abburi, K., Talbott, J. L., Smith, E. D., & Haasch, R. (2008). Removal of arsenic (III) and arsenic (V) from aqueous medium using chitosan-coated biosorbent. *Water Research*, 42, 633-642.

[18] Su, H., Ye, Z., & Hmidi, N. (2017). High-Performance Iron Oxide-Graphene Oxide Nanocomposite Adsorbents for Arsenic Removal. *Colloids and Surfaces A: Physicochemical and Engineering Aspects*, 522, 161–172.

[19] Du, S., Wang, L., Xue, N., Pei, M., Sui, W., & Guo, W. (2017). Polyethyleneimine modified bentonite for the adsorption of amino black 10B. *Journal of Solid State Chemistry*, 252, 152–157.

[20] Uppal, H., Tawale, J., & Singh, N. (2016). Zinc peroxide functionalized synthetic graphite: An economical and efficient adsorbent for adsorption of arsenic (III) and (V). *Journal of Environmental Chemical Engineering*, 4, 2964–2975.